ELSEVIER

Cell Calcium 37 (2005) 565–572

cell calcium

www.elsevier.com/locate/ceca

# Flash photolysis using a light emitting diode: An efficient, compact, and affordable solution

Yann Bernardinelli [a], Christian Haeberli [a], Jean-Yves Chatton [a,b,*]

[a] *Department of Physiology, University of Lausanne, Rue du Bugnon 7, CH-1005 Lausanne, Switzerland*
[b] *Cellular Imaging Facility, University of Lausanne, Switzerland*

Received 17 December 2004; received in revised form 26 February 2005; accepted 3 March 2005
Available online 11 April 2005

**Abstract**

Flash photolysis has become an essential technique for dynamic investigations of living cells and tissues. This approach offers several advantages for instantly changing the concentration of bioactive compounds outside and inside living cells with high spatial resolution. Light sources for photolysis need to deliver pulses of high intensity light in the near UV range (300–380 nm), to photoactivate a sufficient amount of molecules in a short time. UV lasers are often required as the light source, making flash photolysis a costly approach. Here we describe the use of a high power 365 nm light emitting diode (UV LED) coupled to an optical fiber to precisely deliver the light to the sample. The ability of the UV LED light source to photoactivate several caged compounds (CMNB-fluorescein, MNI-glutamate, NP-EGTA, DMNPE-ATP) as well as to evoke the associated cellular $Ca^{2+}$ responses is demonstrated in both neurons and astrocytes. This report shows that UV LEDs are an efficient light source for flash photolysis and represent an alternative to UV lasers for many applications. A compact, powerful, and low-cost system is described in detail.


*Keywords:* Flash photolysis technique; UV LED; Fluorescence; Caged compounds

## 1. Introduction

The flash photolysis technique allows the fast and spatially defined application of bioactive molecules and is therefore a powerful tool for the dynamic study of the molecular mechanisms underlying physiological processes at the cellular level. It can be combined to electrophysiological techniques (e.g. patch-clamp) or cellular imaging techniques (e.g. fluorescence microscopy) to monitor cellular responses to photoactivation of the caged molecules. Caged compounds are composed of active molecules that are covalently bound to a photoabsorbing group resulting in a photolabile, biologically inert molecule. Upon UV illumination, the photolabile caged compound releases the free, biologically active molecule along with the free caging group [1]. Several classes of compounds such as neurotransmitters, nucleotides, $Ca^{2+}$ chelators, fluorescent dyes, or second messengers are commercially available as caged compounds and can be exploited for a wide panel of biological applications [2]. Flash photolysis of caged compounds has many advantages for the study of living cells in real time. For example, caged versions of compounds such as $IP_3$, cyclic AMP or caged $Ca^{2+}$, can be loaded into the cell and released inside the cell. The photochemical reaction is very fast, usually ranging from submicroseconds to milliseconds, and can be triggered at any moment during the course of the experiment in spatially defined regions of the specimen [3].

Caged compounds are photolyzed in the 300–380 nm range of the UV spectrum [3], and require the use of powerful light sources either pulsed or continuous. Xenon [4–6] or mercury [7–10] arc lamps coupled to a electrical or mechanical shutter, as well as flash lamps [11–13] that provide short pulses of UV light, are often used coupled to a microscope via the epifluorescent port, producing uncaging in defined areas [3]. Because high power flash lamps produce large electromagnetic artifacts and need up to several seconds

* Corresponding author. Tel.: +41 21 692 5106; fax: +41 21 692 5105.
*E-mail address:* jean-yves.chatton@unil.ch (J.-Y. Chatton).

0143-4160/$ – see front matter © 2005 Elsevier Ltd. All rights reserved.
doi:10.1016/j.ceca.2005.03.001

to re-charge, they are incompatible with certain experimental approaches as discussed by others [14]. The main advantage of flash lamps or arc lamps is the lower cost compared to UV lasers [3].

Lasers of various types (pulsed frequency tripled Nd:YAG lasers [15], frequency doubled ruby laser [16], nitrogen laser [17,18]), or continuous wave argon laser [17,19]), have been the source of choice for flash photolysis, since their higher luminous density enables them to release caged compounds in small spatial domains using brief pulses of light. Two-photon excitation using femtosecond infrared lasers is also used for flash photolysis [20,21] because it allows releasing caged compound in a diffraction-limited volume at the focal point of objectives [22]. Despite the growing interest for flash photolysis, the high cost of UV lasers and the difficulty of implementing the technique have hindered the widespread use of this technique.

Light emitting diode (LED) could be an alternative UV light source for flash photolysis as recent innovations in the semiconductor industry has seen the production of a device that can emit UV light of wavelengths and powers potentially compatible with photolysis applications. The cost of these devices is considerably lower than UV lasers and flash lamps. In the present report, we demonstrate the feasibility of using a high power UV LED as a light source for flash photolysis with several applications for intracellular calcium ($Ca_i^{2+}$) homeostasis.

## 2. Materials and methods

### 2.1. Cell culture

Cortical astrocytes in primary culture were obtained from 1- to 3-day-old OF1 mice as described previously [23]. Briefly, after microdissection and dissociation of the cortex, cells were grown for 2–5 weeks on 12 mm glass coverslips in DME medium (Gibco) containing 25 mM glucose, and supplemented with 10% FCS, penicillin, streptomycin and amphotericin. Mouse cortical primary cultures of neurons were performed with E17 mouse embryos, as previously described [24,25]. After removing meninges, entire cortices were mechanically dissociated in a phosphate buffer saline (PBS)-glucose solution without divalent cations (100 mM NaCl, 3 mM KCl, 1.5 mM $KH_2PO_4$, 7.9 mM $Na_2HPO_4$, 33 mM glucose, 100 U/ml penicillin and 100 μg/ml streptomycin) and resuspended in Neurobasal-medium (Gibco) containing 2% B27 supplement (Gibco), 0.5 mM glutamine, and 25 μM glutamate. Neurons were then cultured onto poly-ornithine coated coverslips to produce highly enriched cultures of neurons [25]. After 3 h in vitro, the coverslips containing the neurons were placed on top of a feeder layer of cortical glial cells prepared as described above and were allowed to grow for 2–3 weeks. These procedures have been approved by our state legislation and follow their guidelines.

### 2.2. Fluorescence imaging

$Ca_i^{2+}$ was measured using the $Ca^{2+}$-sensitive fluorescent probe Fluo-4. Fluorescence was excited at 490 nm and detected at >520 nm (Omega Optical, Brattleboro, VT, USA). Cell loading was performed at 37 °C using the membrane permeant Fluo4-AM (6 μM, Teflabs) in a HEPES-buffered balanced solution (see composition below). Once loaded with dye, cells were placed in an open chamber (Warner Instruments, Hamden, CT, USA) on the stage of an inverted epifluorescence microscope (Diaphot 300, Nikon, Tokyo, Japan) and observed through a 40 × 1.3 N.A. oil-immersion or a 20 × 0.8 N.A. glycerol-immersion objective lens (Nikon). Fluorescence excitation wavelengths were selected using a fast filter wheel fed to the microscope by a liquid light guide (Sutter Instruments, Novato, CA, USA). Fluorescence was detected using Gen $III^+$ intensified CCD Camera (Video-Scope International, Washington DC, USA). Acquisition and digitization of images, as well as time series, was computer controlled using the software Metafluor (Universal Imaging, Downingtown, PA, USA) running on a Pentium PC computer.

Experimental solutions (pH 7.4) contained (mM): NaCl 135, KCl 5.4, HEPES 20, $CaCl_2$ 1.3, $MgSO_4$ 0.8, $NaH_2PO_4$ 0.78, glucose 5. The solution for dye loading contained 20 mM glucose and supplemented with 0.1% Pluronic F127.

When indicated, cells were loaded with NP-EGTA 8 μM for 30 min in HEPES-buffered balanced solution at 37 °C, washed, replaced in culture medium for 3 h 30 min before experimentation.

### 2.3. Optical tools

The high power UV LED (365 nm/100 mW) model NCCU033 was from Nichia (Tokyo, Japan). The LED was mounted on a custom-built aluminum passive cooler. The optical setup was assembled on the breadboard of an optical table (TMC, Peabody, MA) using a 20 × 0.35 N.A. objective lens (Spindler & Hoyer, Germany) or a pair of 9 × 18 fused silica planoconvex lenses (Edmund Industrial Optics, Barrington, NJ) mounted in a lens holder (Edmund), and a xyz fiber optics holder (Melles Griot, Carlsbad, CA). The fiber used was a polyimide coated fused silica optical fiber (model Optran UV 50/125A, CeramOptec, Bonn, Germany) with high UV transmission (50 μm core/125 μm clad/150 μm jacket/0.22 N.A.) and was cleaved on both ends using a CT-07 high precision cleaver (Fujikura, Tokyo, Japan). Before cleaving, the polyimide jacket was removed over 5 cm by soaking the fiber in boiling 95% sulfuric acid for ∼20 min. The photodiode device used for optical alignment was purchased from Till Photonics (Gräfelfing, Germany).

### 2.4. UV LED driver

A driver for the UV LED was realized (Fig. 1A) with an electronic circuit which was fed by a 9 V external power

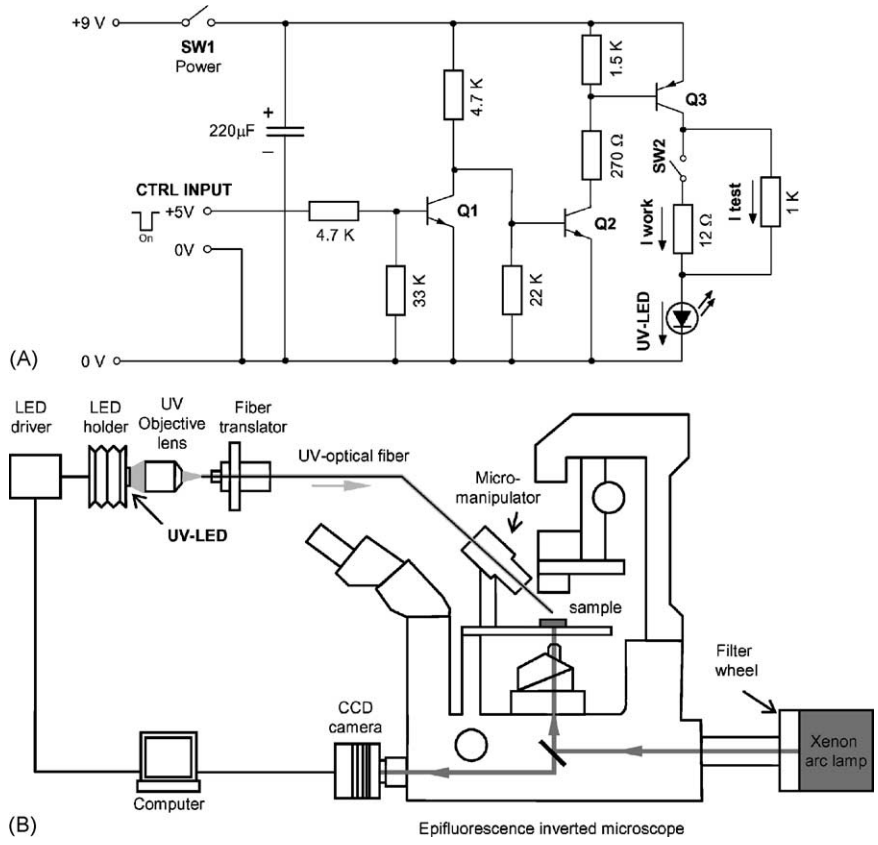


Fig. 1. Scheme of the UV LED system. (A) Diagram of the UV LED driver as described in the text body. (B) Schematic representation of the UV LED assembly coupled to the epifluorescence microscope (see Section 2 and text body for the description).

supply able to provide a 1A dc current. To deliver high power light pulses the switch 2 (SW2) is closed letting a 500 mA current (Iwork) flow through the UV LED. This current represents 70% of the maximum current rating for this UV LED (700 mA). During the adjustment and alignment of the optical assembly SW2 is open, and a test current of 6 mA (Itest) flows through the UV LED. A TTL trigger, sent by the computer to the CTRL input, is used to switch the LED on and off. In this design, pulling the trigger line to 0 V switches the UV LED on, allowing convenient manual control of the driver by using the switch 1 (SW1), even when a computer is not connected. Transistor Q1 inverts the control signal, and Q2 makes a level translation of the pulse for the transistor Q3 which drives the current for the UV LED. The computer parallel port is used as the trigger line controlled through the Metafluor software (Universal Imaging, USA), enabling UV pulses of varying durations to be sent at any moment during the course of the experiment.

### 2.5. Chemicals

4-Methoxy-7-nitroindolinyl-caged L-glutamate (MNI-caged-L-glutamate) was from Tocris-Anawa Trading (Zürich, Switzerland). Fluorescein bis-(5-carboxymethoxy-2-nitrobenzyl) ether dipotassium salt (CMNB-caged fluorescein), *o*-nitrophenyl EGTA-AM (NP-EGTA), adenosine 5′-triphosphate $P^3$-(1-(4,5-dimethoxy-2-nitrophenyl)ethyl) ester disodium salt (DMNPE-caged ATP), and Pluronic F-127 from Molecular Probes (Eugene, OR, USA). All other compounds were from Sigma. Table 1 compares the photolysis quantum efficiency of the compounds used in this study.

Table 1
Photolysis quantum efficiency of tested caged compounds

| Compound name | Quantum efficiency | References |
|---|---|---|
| CMNB-fluorescein | ∼0.13[a] | [32] |
| MNI-glutamate | 0.08 | [11] |
| NP-EGTA | 0.23 | [33] |
| DMNPE-ATP | 0.07 | [34] |

Comparison of quantum yields of the caged compounds tested in this study. Data were compiled from the literature.
[a] Quantum efficiency of the structurally related caged compound CMNB-phenylephrine.

## 3. Results

Several commercially available models of UV LEDs have been tested in our laboratory over the past few years for

their potential usefulness as light source for photolysis. Even though most of them were able to uncage CMNB-caged fluorescein (CMNB-fluorescein), the 100 mW 365 nm UV LED recently released by Nichia was the first to combine the adequate wavelength and power for flash photolysis applications. Therefore, this report will focus on this particular UV LED model.

### 3.1. Setup configuration

In a first phase, a driver for the UV LED was realized (Fig. 1A) that uses a 9 V external power supply. The driver is either manually controlled or driven by means of TTL pulses to generate UV pulses of varying durations at any time during the course of an experiment. The UV LED was mounted on an aluminum passive cooler to dissipate the heat generated by the relatively high current used for light pulses (Fig. 1B). The light was focused on a multimode fused silica 50 μm core optical fiber mounted in a xyz fiber optics holder by using a 20 × 0.35 N.A. microscope objective lens (Fig. 1B) or two planoconvex fused silica lenses (*not shown*). The fine optical alignment was optimized by monitoring the light output at the fiber exit using a photodiode. The optical fiber was positioned at ∼45° in the field of view using a micromanipulator (Fig. 1B).

### 3.2. CMNB-caged fluorescein uncaging efficiency

The ability of the UV LED flash photolysis system to photoactivate CMNB caged-fluorescein was first tested. This compound is not fluorescent until photoactivation releases the brightly fluorescent fluorescein molecule. CMNB-caged fluorescein (100 μM) was dissolved in 100% glycerol to limit the diffusion of released fluorescein and allow the precise observation of the photoactivated area. The fiber tip was placed in the glycerol drop deposited on a glass coverslip approximately 20 μm above the glass surface. UV light flashes of 100, 500, and 1000 ms were delivered through the fiber and resulted in stepwise increases in fluorescence intensity in the flashed area (Fig. 2A) monitored by excitation at 490 nm (emission >520 nm) of photoreleased fluorescein through the epifluorescence microscope.

Images of the flashed area, represented in pseudocolor scale in Fig. 2B, acquired ∼100 ms after the UV flash show that the amount of fluorescein released is proportional with the duration of photolysis. Fig. 2B shows that the elliptic

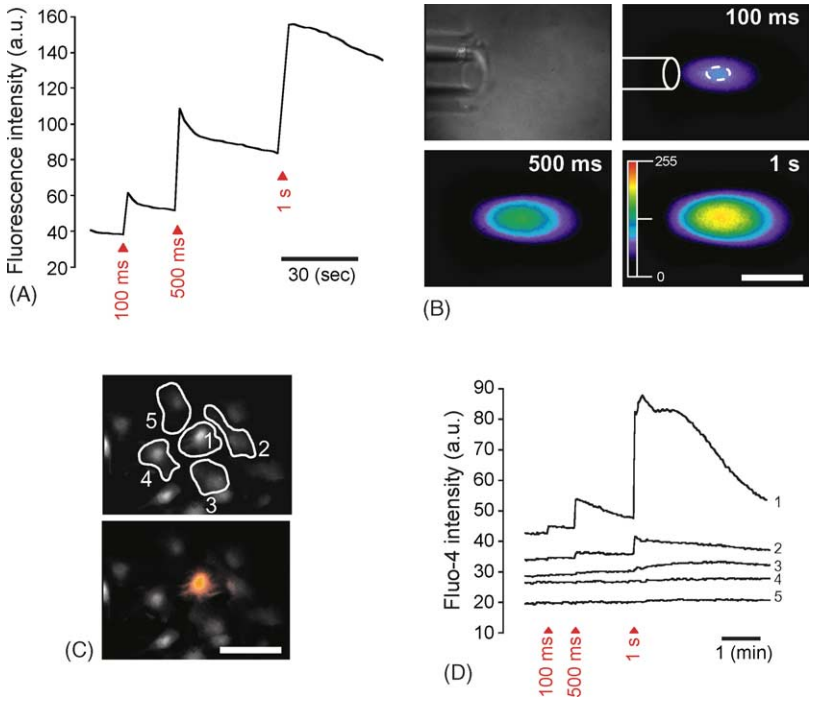


Fig. 2. Initial testing of UV LED flash photolysis. (A) Fluorescence intensity of photoreleased fluorescein plotted against time. Three consecutives UV flashes of 100, 500 and 1000 ms (red arrows) were delivered from the UV LED through the optical fiber placed in a glycerol drop containing CMNB-caged fluorescein (100 μM) on the microscope stage. (B) Transmitted light image of the cleaved optical fiber tip in the glycerol drop (top left). The inner core of the fiber was drawn and overlaid in the top right image (plain white lines). The three pseudocolor images show the 2D distribution of the uncaged fluorescein after the three consecutive UV stimuli, depicting different areas of fluorescence intensity. The 100 ms flash (top right) allowed us to trace (white stripped line) the full-width-half-maximal intensity area. Representative results out of nine separate experiments. (C) $Ca^{2+}$ uncaging performed in astrocytes loaded with the caged $Ca^{2+}$ compound NP-EGTA and the $Ca^{2+}$ probe Fluo-4 (top image). The mask drawn in (B) was aligned with the fiber inner core and used to aim the UV beam at cell 1. The false color overlay in the bottom image shows that only the targeted cell 1 exhibited a significant elevation of cytosolic $Ca^{2+}$. (D) Fluo-4 fluorescence intensities plotted against time, showing that repetitive $Ca_i^{2+}$ responses can be triggered by NP-EGTA uncaging in the five selected cells indicated in the top image of (C). Scale bar 100 μm. Representative experiment out of five.

area of photoactivation, corresponding to the area of full-width-half maximum (FWHM) intensity, had a size of $33.4 \pm 1.2$ μm (small diameter) and $62.7 \pm 3.6$ μm (large diameter) located $\sim 54 \pm 7$ μm away from the fiber tip. This area corresponds to the highest intensity of UV light output, which is about the size of a cultured astrocyte. The outline of the inner fiber tip end from transmitted image and the outline of the FWHM intensity area were then drawn to create a mask (Fig. 2B, top left) used to help aiming the UV beam at distinct cells in the field of view in subsequent protocols.

### 3.3. Determination of the spatial accuracy of uncaging using NP-EGTA

We then asked whether this system was able to uncage bioactive compounds and whether it was able to target a single cell. The caged $Ca^{2+}$ compound NP-EGTA, a $Ca^{2+}$ chelator, can be loaded into the cell using its membrane-permeant derivative NP-EGTA AM. Photoactivation of NP-EGTA causes the fragmentation of the molecule in two parts having negligible $Ca^{2+}$ affinities, resulting in fast $Ca^{2+}$ release [3]. This caged compound has been extensively used to study $Ca^{2+}$ signaling [5,9,18,19,26]. Cultured cortical mouse astrocytes were simultaneously loaded with NP-EGTA (30 min, 8 μM) and the $Ca^{2+}$ fluorescent indicator Fluo4-AM, allowing the monitoring of intracellular $Ca^{2+}$ change after photolysis. The fiber tip was placed 20 μm above the cell surface and positioned within the mask as described above. A selected cell in the field of view was placed in the area corresponding to the highest intensity defined by the mask. Cells were then flashed and the $Ca_i^{2+}$ changes were monitored against time in the aimed cell as well as in the surrounding cells (Fig. 2D). Fig. 2C shows a clear $Ca_i^{2+}$ increase in the aimed cell after flashes of 100, 500 ms and 1 s. Very weak $Ca^{2+}$ increases could be observed in neighboring cells (e.g. cells 2 and 3) after 500 ms and 1 s flashes. However, no detectable increase over basal $Ca_i^{2+}$ could be observed for shorter (100 ms) flashes (Fig. 2D). It is not certain whether the small $Ca_i^{2+}$ elevation in the neighboring cells is due to direct $Ca^{2+}$ uncaging or to the propagation of a $Ca_i^{2+}$ elevation from the targeted cell as a wave [27,28]. Nevertheless, these experiments indicate that in the present configuration, the precision of the method is at the level of a single cell.

### 3.4. Application to MNI-caged glutamate and DMNPE-caged ATP

MNI-caged glutamate (MNI-glu) is an inert, stable and rapidly released caged neurotransmitter [29] that has been used, for instance, to mimic the synaptic input and map the glutamate sensitivity of the dendritic tree of neurons [30]. Astrocytes express metabotropic glutamate receptors (mGluRs) [31] coupled to inositol phosphate/$Ca^{2+}$ signal transduction pathway. MNI-glu (1 mM) was added to the bath of astrocytes

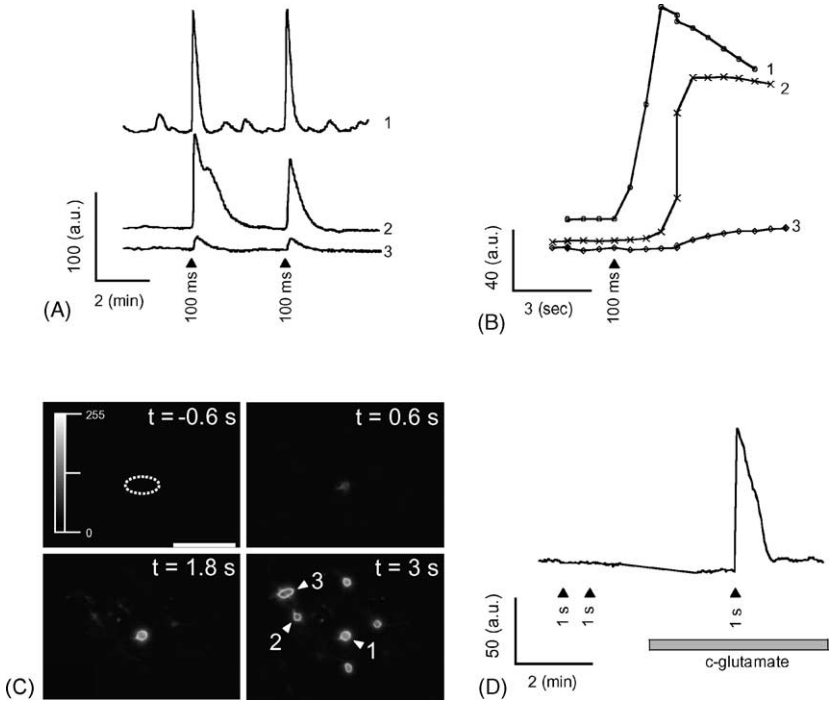


Fig. 3. Astrocytic response to the extracellular uncaging of MNI-caged glutamate.(A) Fluo-4 fluorescence plotted against time, showing that repetitive $Ca_i^{2+}$ responses can be triggered by glutamate uncaging (100 ms flashes) in three selected cells indicated in the last image of C. (B) Zoomed up traces of the graph A, showing the sequential pattern of response in the three cells. (C) A gallery of Fluo-4 fluorescence images. The initial image has been subtracted from all the images, which show the extension of the $Ca^{2+}$ response as a wave. The top image recorded −0.6 s before photoactivation indicates the region where UV light spot was applied (i.e. cell 1). Representative experiments out of six. Scale bar 100 μm. (D) One-second UV flashes in the absence of caged compound in the bath did not produce any response from the cells ($n = 7$ experiments).

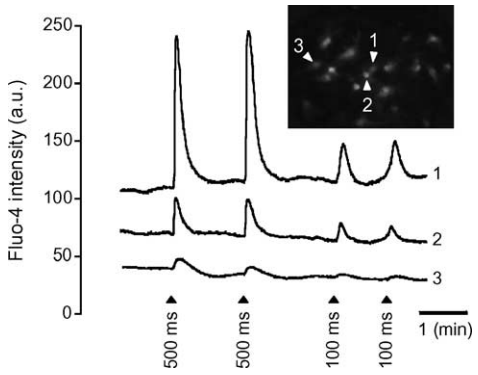


Fig. 4. Uncaging of DMNPE-caged ATP. The graph shows Fluo-4 fluorescence plotted against time. Repetitive $Ca_i^{2+}$ responses can be triggered by ATP uncaging (two 500 ms and two 100 ms flashes) in three selected astrocytes indicated in the image (cell 1 is the aimed cell). Representative experiment out of eight.

loaded with the $Ca^{2+}$ probe Fluo-4. The fiber was placed 20 μm above the cell monolayer and aimed at one single cell. Fig. 3A shows that by photoactivation (100 ms) of extracellular MNI-glu on one single cell, resulted in an increase in $Ca_i^{2+}$ in the aimed cell as well as in surrounding cells. Focal application of glutamate and several other neurotransmitters are known to initiate the spreading of $Ca^{2+}$ waves [27]. By carefully looking at the time course of the $Ca_i^{2+}$ increase a shift is observed between the onset of the response in the targeted cell and the cells more distant from photolysis spot (Fig. 3B). In fact, the $Ca_i^{2+}$ rise occurred in a cell-by-cell manner like a wave starting from the cell stimulated by flash photolysis (Fig. 3C and D). Similar results have been observed by others when a different type of caged glutamate (CNB-glutamate) is photoreleased onto astrocytes [17].

DMNPE-caged ATP (caged ATP) is an inactive and photolabile precursor of ATP and has been used for neuronal studies [8]. Astrocytes express P2Y purinergic receptors, a family of G-protein-coupled receptors activated mainly by ATP whose activation leads to robust $Ca^{2+}$ responses. One astrocyte was flashed with the presence of exogenous caged ATP (1 mM). A $Ca_i^{2+}$ response of the same type as with caged glutamate was observed in the aimed astrocyte and at a lesser extent in the surrounding cells (Fig. 4).

In the absence of MNI-glu (Fig. 3D) or DMNPE-caged ATP (*not shown*) in the extracellular bath, no $Ca_i^{2+}$ increase were induced by the UV flashes, excluding that the $Ca^{2+}$ responses were due to a direct effect of the UV stimulation on the cells.

Taken together, these results indicate that the LED UV light is not only applicable to intracellular uncaging, but also to extracellular photolysis of bioactive compounds.

### 3.5. Determination of the minimal pulse duration

We then asked whether the pulse duration could be reduced under 100 ms. Neurons being more sensitive to glutamate than cultured astrocytes, their response to glutamate photorelease was tested under the same conditions in order to determine the efficiency of the LED photolysis approach. $Ca_i^{2+}$ increase in the aimed neurons was monitored using Fluo-4 after flashes of 1, 5, 10, and 50 ms in the presence of 1 mM MNI-glu. Fig. 5 shows that a 1 ms pulse already induced a detectable $Ca^{2+}$ response in the aimed

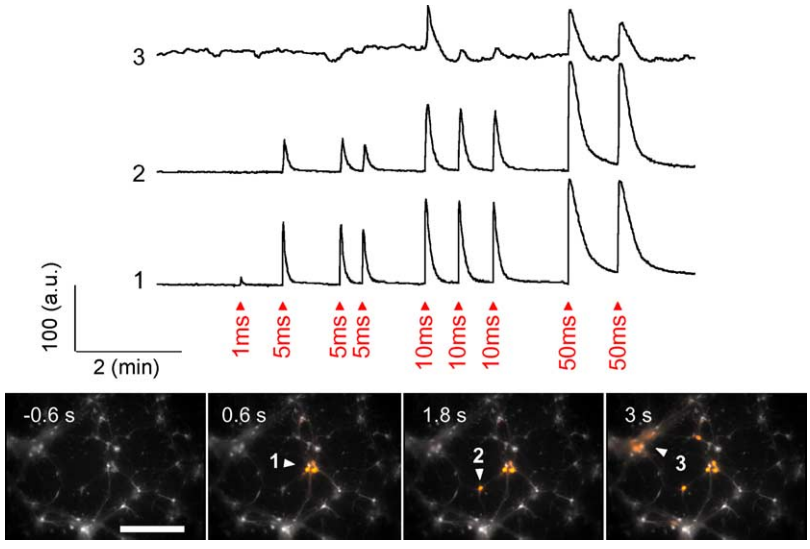


Fig. 5. Neuronal stimulation using MNI-caged glutamate. Graphs show neuronal Fluo-4 fluorescence plotted against time for three different regions indicated by the arrow heads in the image series. A 1 ms flash triggered a modest $Ca_i^{2+}$ response in the aimed neurons (region 1) following glutamate photorelease. By applying a 5 ms flash, two groups of neurons (1 and 2) exhibited a $Ca_i^{2+}$ increase. The delivering of both 10 and 50 ms pulses induced a stronger $Ca_i^{2+}$ response and several neurons were activated. The images represent a time series of Fluo-4 loaded neurons and show the extension of the $Ca_i^{2+}$ response from the photoactivated neurons to the other neurons. The basal $Ca_i^{2+}$ level is represented in a gray scale and the $Ca_i^{2+}$ elevation due to the photoactivation in an orange scale. Representative experiments out of four. Scale bar 200 μm.

neurons, and that 5 ms pulses initiated a multi-neuronal response.

Taken together, these results show that a high power UV LED used for flash photolysis is an efficient UV light source. The four caged compounds tested were photoactivated by pulses as short as 1 ms in areas of single cell size delivered using an optical fiber.

## 4. Discussion

LEDs were first introduced commercially in the 1960s and emitted infrared and then red light. From that point on, the semiconductor industry has put enormous efforts in the development of LEDs with always shorter wavelengths and with improved efficiency and power. The most recent innovations in the LED technology are devices that can emit UV light.

The material used for manufacturing the semiconductor core of modern LEDs, which determines the wavelength of emitted light, is usually a combination of gallium, arsenic and phosphorus. However, these materials present a problem in that efficiency of light production is rapidly degraded at wavelengths shorter than 380 nm because self-absorption of gallium nitride layers. Recently, a UV LED was developed without gallium nitride layer which can provide high light outputs even at short wavelength. In particular, a high power 365 nm UV LED has been successfully produced with an output power of 100 mW.

We show in the present study that this type of UV LED provide enough energy to efficiently uncage the four caged compounds tested here, namely: caged glutamate, caged ATP, caged $Ca^{2+}$, and caged fluorescein, which have quantum yields ranging from 0.07 to 0.23 (Table 1).

UV light is often delivered through the microscope objective for photolysis applications. Parpura and Haydon [14] have proposed the utilization of an optical fiber to deliver the laser UV light directly to the sample. The fiber optics approach offers, however, important advantages, for instance in neuroscience research because it allows uncaging compounds away from the field of view where imaging or electrical recording is performed. It is also a device that is not physically attached to a given microscope and can be readily transported to other experimental setups. However, the use of fiber optic light delivery cannot match the spatial accuracy that can be achieved using high numerical aperture microscope objectives. Nevertheless, the use of small or tapered fibers [14] allows restricting the illuminated spot to acceptable sizes. However, when necessary, UV LED light beam could also be directed through the objective lens.

The adequacy of LEDs, arc lamps, or lasers for UV flash photolysis will strongly depend on how the UV light is to be delivered to the sample as well as on the size of the photoactivated area at the specimen plane. Thus, although a side-by-side comparison of the UV LED performance with other sources would be informative, it is difficult to achieve because the spectral bandwidth, dimension and light intensity distribution of the produced light spot are quite different among sources. The present study, however, demonstrates that high power UV LEDs are efficient UV light sources for flash photolysis able to uncage several different caged compounds, with uncaging durations as short as 1–5 ms. As in the configuration presented, the illuminated spot had the size of a cell, the advantages of flash photolysis for rapid and spatially controlled delivery of bioactive compounds can be fulfilled using UV LEDs. This approach is therefore a realistic alternative to UV lasers and arc lamps and should be applicable to numerous experimental situations with the additional advantages of low cost, portability, and simplicity of implementation.

## Acknowledgements

The authors wish to thank Michel Saint-Ghislain for his help with fiber cleaving, to Benjamin Rappaz for providing neuron cultures, and to Graham W. Knott for his reading of the manuscript. This work was supported by SNF grant #3100-067116 to J.-Y.C.

## References

[1] K. Kandler, R.S. Givens, L.C. Katz, Photostimulation with caged glutamate, in: R. Yuste, F. Lanni, A. Konnerth (Eds.), Imaging Neurons, A Laboratory Manual, New-York, Cold Spring Harbor Laboratory Press, 2000, pp. 27.21–27.29.
[2] J.M. Nerbonne, Caged compounds: tools for illuminating neuronal responses and connections, Curr. Opin. Neurobiol. 6 (1996) 379–386.
[3] G.C.R. Ellis-Davies, Basics of photoactivation, in: R. Yuste, F. Lanni, A. Konnerth (Eds.), Imaging Neurons, A Laboratory Manual, Cold Spring Harbor Laboratory Press, New York, 2000, pp. 24.21–24.28.
[4] G.D. Housley, N.P. Raybould, P.R. Thorne, Fluorescence imaging of $Na^+$ influx via P2X receptors in cochlear hair cells, Hear Res. 119 (1998) 1–13.
[5] M. Kreft, M. Stenovec, M. Rupnik, et al., Properties of $Ca^{2+}$-dependent exocytosis in cultured astrocytes, Glia 46 (2004) 437–445.
[6] T. Haller, K. Auktor, M. Frick, N. Mair, P. Dietl, Threshold calcium levels for lamellar body exocytosis in type II pneumocytes, Am. J. Physiol. 277 (1999) 893–900.
[7] R. Dumollard, K. Hammar, M. Porterfield, et al., Mitochondrial respiration and $Ca^{2+}$ waves are linked during fertilization and meiosis completion, Development 130 (2003) 683–692.
[8] B.V. Zemelman, N. Nesnas, G.A. Lee, G. Miesenbock, Photochemical gating of heterologous ion channels: remote control over genetically designated populations of neurons, Proc. Natl. Acad. Sci. U.S.A. 100 (2003) 1352–1357.
[9] L. Leybaert, K. Paemeleire, A. Strahonja, M.J. Sanderson, Inositol-trisphosphate-dependent intercellular calcium signaling in and between astrocytes and endothelial cells, Glia 24 (1998) 398–407.
[10] S. Iwabuchi, K. Kawahara, K. Makisaka, H. Sato, Photolytic flash-induced intercellular calcium waves using caged calcium ionophore in cultured astrocytes from newborn rats, Exp. Brain. Res. 146 (2002) 103–116.
[11] G. Papageorgiou, J.E.T. Corrie, Effects of aromatic substituents on the photocleavage of 1-acyl-7-nitroindolines, Tetrahedron 56 (2000) 8197–8205.
[12] G. Rapp, K. Guth, A low cost high intensity flash device for photolysis experiments, Pflugers Arch. 411 (1988) 200–203.

[13] J.Y. Chatton, Y. Cao, J.W. Stucki, Perturbation of myo-inositol-1,4,5-trisphosphate levels during agonist-induced $Ca^{2+}$ oscillations, Biophys. J. 74 (1998) 523–531.
[14] V. Parpura, P.G. Haydon, UV photolysis using a micromanipulated optical fiber to deliver UV energy directly to the sample, J. Neurosci. Methods 87 (1999) 25–34.
[15] P. Xia, P.M. Bungay, C.C. Gibson, O.N. Kovbasnjuk, K.R. Spring, Diffusion coefficients in the lateral intercellular spaces of Madin-Darby canine kidney cell epithelium determined with caged compounds, Biophys. J. 74 (1998) 3302–3312.
[16] B. Zimmermann, A.V. Somlyo, G.C. Ellis-Davies, J.H. Kaplan, A.P. Somlyo, Kinetics of prephosphorylation reactions and myosin light chain phosphorylation in smooth muscle. Flash photolysis studies with caged calcium and caged ATP, J. Biol. Chem. 270 (1995) 23966–23974.
[17] J.Y. Sul, G. Orosz, R.S. Givens, P.G. Haydon, Astrocytic connectivity in the hippocampus, Neuron Glia Biol. 1 (2004) 3–11.
[18] Q.S. Liu, Q. Xu, G. Arcuino, J. Kang, M. Nedergaard, Astrocyte-mediated activation of neuronal kainate receptors, Proc. Natl. Acad. Sci. U.S.A. 101 (2004) 3172–3177.
[19] T. Fellin, O. Pascual, S. Gobbo, T. Pozzan, P.G. Haydon, G. Carmignoto, Neuronal synchrony mediated by astrocytic glutamate through activation of extrasynaptic NMDA receptors, Neuron 43 (2004) 729–743.
[20] S.J. Mulligan, B.A. MacVicar, Calcium transients in astrocyte endfeet cause cerebrovascular constrictions, Nature 431 (2004) 195–199.
[21] M. Matsuzaki, G.C. Ellis-Davies, T. Nemoto, Y. Miyashita, M. Iino, H. Kasai, Dendritic spine geometry is critical for AMPA receptor expression in hippocampal CA1 pyramidal neurons, Nat. Neurosci. 4 (2001) 1086–1092.
[22] D.L. Pettit, S.S. Wang, K.R. Gee, G.J. Augustine, Chemical two-photon uncaging: a novel approach to mapping glutamate receptors, Neuron 19 (1997) 465–471.
[23] O. Sorg, P.J. Magistretti, Vasoactive intestinal peptide and noradrenaline exert long-term control on glycogen levels in astrocytes: blockade by protein synthesis inhibition, J. Neurosci. 12 (1992) 4923–4931.
[24] G.J. Brewer, Serum-free B27/neurobasal medium supports differentiated growth of neurons from the striatum, substantia nigra, septum, cerebral cortex, cerebellum, and dentate gyrus, J. Neurosci. Res. 42 (1995) 674–683.
[25] G.J. Brewer, J.R. Torricelli, E.K. Evege, P.J. Price, Optimized survival of hippocampal neurons in B27-supplemented Neurobasal, a new serum-free medium combination, J. Neurosci. Res. 35 (1993) 567–576.
[26] A. Araque, R.P. Sanzgiri, V. Parpura, P.G. Haydon, Calcium elevation in astrocytes causes an NMDA receptor-dependent increase in the frequency of miniature synaptic currents in cultured hippocampal neurons, J. Neurosci. 18 (1998) 6822–6829.
[27] A.C. Charles, C. Giaume, Intercellular calcium waves in astrocytes: underlying mechanisms and functional significance, in: A. Volterra, P.J. Magistretti, P.G. Haydon (Eds.), The Tripartite Synapse, Oxford University Press, New York, 2002, pp. 110–126.
[28] Y. Bernardinelli, P.J. Magistretti, J.Y. Chatton, Astrocytes generate $Na^+$-mediated metabolic waves, Proc. Natl. Acad. Sci. U.S.A. 101 (2004) 14937–14942.
[29] M. Canepari, L. Nelson, G. Papageorgiou, J.E. Corrie, D. Ogden, Photochemical and pharmacological evaluation of 7-nitroindolinyl- and 4-methoxy-7-nitroindolinyl-amino acids as novel, fast caged neurotransmitters, J. Neurosci. Methods 112 (2001) 29–42.
[30] E.M. Callaway, R. Yuste, Stimulating neurons with light, Curr. Opin. Neurobiol. 12 (2002) 587–592.
[31] G.P. Schools, H.K. Kimelberg, mGluR3 and mGluR5 are the predominant metabotropic glutamate receptor mRNAs expressed in hippocampal astrocytes acutely isolated from young rats, J. Neurosci. Res. 58 (1999) 533–543.
[32] G.P. Ahern, S.F. Hsu, M.B. Jackson, Direct actions of nitric oxide on rat neurohypophysial $K^+$ channels, J. Physiol. 520 (Pt. 1) (1999) 165–176.
[33] G.C. Ellis-Davies, J.H. Kaplan, Nitrophenyl-EGTA, a photolabile chelator that selectively binds $Ca^{2+}$ with high affinity and releases it rapidly upon photolysis, Proc. Natl. Acad. Sci. U.S.A. 91 (1994) 187–191.
[34] J.F. Wooton, D.R. Trentham, 'Caged' compounds to probe the dynamics of cellular processes: synthesis and properties of some novel P-2-photosensitive P-2-nitrobenzyl esters of nucleotides, in: P.E. Nielsen (Ed.), Photochemical Probes in Biochemistry, Kluwer Academic Publishers, Dordrecht, 1989, pp. 277–296.